Turkish J. Eng. Env. Sci.
26 (2002) , 49 – 58.

Modeling of Radiative Heat Transfer in the Freeboard of a Fluidized Bed Combustor Using the Zone Method of Analysis

Aykan BATU and Nevin SELÇUK
Department of Chemical Engineering,
Middle East Technical University,
06531 Ankara, TURKEY
e-mail: selcuk@metu.edu.tr

Received 21.09.2001

Abstract

Radiative heat transfer in the freeboard of the METU 0.3 MW_t atmospheric bubbling fluidized bed combustor (ABFBC) test rig was analyzed by applying one of the most accurate radiation models, the zone method of analysis, to the prediction of incident radiative heat fluxes on the side walls. The accuracy of the method was tested by comparing its predictions with measured incident radiative fluxes on the walls. The freeboard was treated as a 3-D rectangular enclosure containing gray, absorbing, emitting and isotropically scattering medium. Data for application and validation were generated from METU 0.3 MW_t ABFBC burning lignite in its own ash. Comparisons revealed that the zone method of analysis reproduces the wall fluxes in the freeboard of fluidized bed combustors containing particle-laden combustion gases reasonably well. The sensitivity of predicted heat fluxes to the presence of particles was also examined and found to be insensitive at low particle loads typical of bubbling fluidized bed combustors.

Key Words: zone method of analysis, radiative heat transfer in freeboard, fluidized bed coal combustion

Introduction

Radiative heat transfer in an absorbing, emitting, scattering medium is an important aspect in many practical engineering problems such as the modeling of energy transport in combustion chambers and furnaces. In fluidized bed combustion, the efficiency depends upon the heat recovered in the freeboard region, where the dominant component of heat transfer is radiation to which the major contributor is the emittance from combustion off-gases and fly-ash particles. Therefore, the modeling of the radiative heat transfer in such systems necessitates an accurate knowledge of the radiative properties of the particle-laden combustion gases. Calculation of the radiative properties, on the other hand, requires information on temperatures and gas composition as well as particle concentration, composition, shape and size distribution.

Difficulties encountered in obtaining such data from industrial scale units lead to the use of small scale test rigs equipped for measurements. A pioneering study on the measurement of the emissivity and transmissivity of particle-laden combustion gases in the freeboard of a simulated atmospheric bubbling fluidized bed combustor (ABFBC), where silica sand is fluidized in propane-air combustion products, has been performed by Lindsay et al. (1986). It was reported that the dominant component of heat transfer is radiation from particle-laden combustion gases. The investigation was extended to the prediction of the effect of scattering on the emissivity of the particle hold up in the freeboard of a 1 MW_t ABFBC burning coal with and without limestone addition in a bed of sand particles by Filla et al. (1996). Predictions of particle cloud emissivity have shown a significant effect of scattering on the radiative properties of particle-laden flue gases.

An extensive experimental study in an ABFBC

providing data required both for the calculation of radiative properties and for the assessment of the accuracy of the radiative heat exchange models was performed by Kozan and Selçuk (2000). Data on flow rates, concentrations and temperatures together with incident radiative heat fluxes in the freeboard of a 0.3 MW_t ABFBC burning lignite in its own ash were measured during the steady state operation of the rig. Radiative exchange in the freeboard of the combustor was modeled by using a simple engineering approach, i.e. a well-stirred enclosure model in conjunction with the Radiosity-Irradiation Method (RIM) and radiative properties of particle-laden combustion gases estimated from measured data. Significant discrepancies between the predicted and measured incident radiative fluxes were observed. This was considered to be due to the single zone treatment of the freeboard in which a constant uniform incident heat flux was used to represent the relatively steep variation of the measured profile along the freeboard wall. Therefore, more sophisticated radiation models must be applied for the analysis of radiative transfer in the freeboard.

The basis of all radiation models is the Radiative Transfer Equation (RTE), which has the form of an integro-differential equation and as such is not amenable to analytical solution. Hence, many approximate solution methods have been proposed. These methods can be broadly classified into two groups. The first group is based on discretizing the continuous angular variation of intensity into a finite number of directions and hence the transformation of RTE into a set of differential equations. Multiflux, discrete ordinates, and finite volume methods are some of the examples within this group. The second group, comprising Hottel's zone method and the Monte Carlo method, on the other hand, make no approximation or assumption to simplify the RTE. Utilizing the concept of radiosity and the principle of conservation of energy, Hottel's zone method transforms the RTE into a set of algebraic equations.

In this method, the enclosure is subdivided into a finite number of isothermal volume and surface area zones. An energy balance is then performed for the radiative heat exchange between any zone and every other zone using precalculated 'exchange areas'. This process leads to a set of simultaneous equations for the unknown temperatures or heat fluxes. Accuracy assessment studies to date have shown that it is one of the most accurate methods in predicting heat flux distributions and temperatures.

Therefore, the objective of this study was to analyze the radiative heat transfer in the freeboard of the 0.3 MW_t ABFBC test rig containing particle-laden combustion gases by applying the zone method of analysis. Steady state operating data on flow rates, medium and wall temperature distributions, and gas composition as well as particle concentration, composition, shape and size distribution were used for the calculation of the radiative properties of the particle-laden combustion gases. The predictive accuracy of the method is assessed by comparing its predictions with incident fluxes measured on the freeboard walls. Variations in predictive accuracy and CPU time with number of zones were also studied. The sensitivity of heat fluxes to the presence of particles and the contribution of particle radiation to the radiative exchange within the freeboard were also examined.

Description of the Test Rig

The main body of the test rig is a modular combustor formed by five modules 1 m in height and with an internal cross-section of 0.45 m x 0.45 m. The first and the fifth modules refer to bed and cooler, respectively, and the three in between are the freeboard modules. There are two cooling surfaces of 0.35 m^2 and 4.3 m^2 in the bed and cooler modules, respectively. At various heights along the combustor, there are 14 ports for thermocouples and 10 ports for gas sampling probes, into which a radiation probe is also inserted. The inner walls of the combustor are lined with alumina-based refractory bricks 6 cm thick. In order to measure the concentrations of O_2, CO, CO_2, SO_2 and NO/NO_x along the combustor at steady state, combustion gas is sampled from the combustor and passed through a gas conditioning system where the sample is filtered, dried and cooled to be fed to the analyzers. The process values such as the flow rates and temperatures of each stream, gas composition and temperature along the combustor are logged to a PC by means of a data acquisition and control system, Bailey INFI 90. Further details concerning the test rig can be found elsewhere (Batu, 2001).

Radiative heat fluxes incident on the refractory side-walls of the freeboard were measured by a Medtherm 48P-20-22K heat flux transducer during the steady state operation of the test rig. The radiometer eliminates the effects of convection and measures only the incident radiative heat flux. The radiometer probe was inserted into the gas sampling ports at five different heights along the freeboard,

flush with the inner surface of the refractory sidewall. The radiometer output for incident radiative heat flux was read from a voltmeter and the readings were then converted to heat fluxes using the certified calibration of the transducer.

The steady state operating conditions required for the radiative property estimation are presented in Table 1. Temperature measurements were carried out on a discrete grid of points along the freeboard at steady state operation. In order to facilitate the use of these measurements as input data in the calculation of radiative exchange, the experimental data were represented by the high order polynomials given in Figure 1. For radiative property estimation of particle-laden combustion gases, particles collected from the cyclone downstream of the freeboard were subjected to particle size distribution analysis by laser light scattering (Göğebakan, 2000).

Zone Method of Analysis

The well-stirred enclosure model is limited in that only overall furnace performance can be predicted. A detailed prediction of heat flux distribution throughout industrial and utility furnaces can be made using the zone method of analysis originally proposed by Hottel and Cohen (1958), in which the enclosure is subdivided into many volume and surface zones. The properties of each zone are considered uniform and constant, and the radiative exchange factors are determined based on the relative orientation of zones and the attenuation coefficient of participating species in each zone. Energy balance equations are written for each zone, resulting in a system of algebraic non-linear equations in terms of the temperature of each zone, allowing the radiative heat flux distribution to be predicted.

In the analysis of radiative transfer by the zone method, the evaluation of radiative exchange factors (generally called exchange areas) for each pair of zones is the most important step. The exchange areas must be evaluated before the energy balances are carried out.

Energy balances, in terms of these exchange areas, for each zone, consider the radiative exchange of the zone with every other zone including itself. The total number of equations and unknowns in the resulting equation set is equal to the total number of zones.

The zone method remains the most widely used method for radiative heat transfer analysis in industrial furnaces due its mathematical simplicity. It has a wide range of applications in energy generation systems, it exhibits the ability to predict real gas behavior in multi- dimensional systems, and it has been successfully employed in problems involving absorbing, emitting and isotropically scattering medium bounded by diffuse reflecting surfaces (Smith et al., 1985; Truelove, 1974; Viskanta and Mengüç, 1987).

Table 1. Operating Conditions for the Experiment

Superficial velocity, u_o(m/s)	3.1
Carryover flow rate, F_c (kg/h)	25
Particle density, ρ_p (kg/m^3)	536.7
Sauter mean diameter, D_{32} (μm)	35.6
Particle load, B (kg/m^3)	0.01
Mass specific cross section, A_{mc} (m^2/kg)	78.6
Average H_2O concentration (%)	10
Average CO_2 concentration (%)	10
Average medium temperature ($^\circ$ C)	890
Mean beam length, L_m (m)	0.38

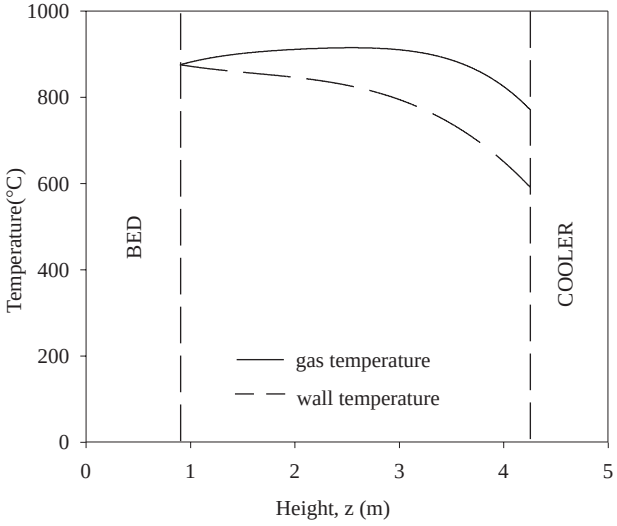

Figure 1. Temperature profiles along the freeboard. Polynomials for temperature profiles; T_g (z) = -5.2962 z^4 + 43.956 z^3 – 146.52 z^2 + 240.79 z + 748.6 [$^\circ$ C], T_w (z) = -11.164 z^3 + 54.123 z^2 – 109.95 z + 938.8 [$^\circ$ C]

Direct exchange areas

Radiative exchange factors between two zones comprising the relative orientation of any zone pairs and allowance for beam attenuation within the medium between the pairs are called direct exchange areas. They are calculated for each pair of zones; surface to surface, gas to surface, surface to gas and gas

to gas. The direct exchange area between two black surfaces i and j is given by

$$s_i s_j = \int_{A_j}\int_{A_i} e^{-\beta L}\frac{\cos\theta_i \cos\theta_j}{\pi L^2} dA_i \cdot dA_j \qquad (1)$$

where β is the extinction coefficient of the medium between the surfaces separated by a distance L, θ's are the angles between the beam joining the zone centers and normals of the zones, and A denotes the area of a surface zone. Equations for surface-volume and volume-volume direct exchange areas are similar and can be found elsewhere (Hottel and Sarofim, 1967).

The multiple integrals defining the direct exchange areas between two finite surface or volume zones can not be integrated analytically when there is a participating medium in between. For the evaluation of direct exchange areas, the surface and volume zones are further subdivided into smaller volume and surface elements and direct numerical integration is carried out by simple summation of the exchange areas between these smaller elements (Rhine and Tucker, 1991, ch.12; Tucker, 1986)

$$s_i s_j = \sum_{j=1}^{N}\sum_{i=1}^{M} \frac{1}{\pi L^2}\cdot\tau(L)\cdot\cos\theta_i\cdot\cos\theta_j\cdot dA_i\cdot dA_j \qquad (2)$$

L now represents the separation between the smaller elements and dA's are the corresponding areas. θ's are the angles between the beam joining the elements and the normals of the surface elements. For instance, for calculating the direct exchange area between surface zones i and j, the areas of i and j are subdivided into M and N equal-sized small elements. The direct exchange area between surface zones i and j, $s_i s_j$, is then obtained by calculating the direct exchange areas between the first element of zone j (j=1) and all elements of zone i (i=1,M), repeating this procedure for the remaining N-1 elements of zone j and summing them. Surface-volume and volume-volume direct exchange areas are evaluated similarly.

Although the reduction in the size of the elements for high accuracy requires large computing times, introducing maximum symmetry into the zoning of the geometrical system avoids repeated calculation for the zone pairs with the same relative orientation (Vercammen and Froment, 1980). From the definition of direct exchange areas, reciprocity requires the following equalities, which also decrease the computational time.

$$s_i s_j = s_j s_i \qquad (3)$$

$$s_i g_j = g_j s_i \qquad (4)$$

$$g_i g_j = g_j g_i \qquad (5)$$

Radiative energy balances

For an enclosure subdivided into m volume and n surface zones, a radiant energy balance is written for each zone (Noble, 1975). For surface zones, it takes the following form:

$$A_i H_i = \sum_{j=1}^{n}(s_i s_j)W_j + \sum_{j=1}^{m}(s_i g_j)W_{g,j} \qquad (6)$$

where

$$W_j = \varepsilon_j E_j + \rho_j H_j \qquad (7)$$

$$W_{g,j} = (1-\omega_o)E_{g,j} + \omega_o H_{g,j} \qquad (8)$$

In Equation (6), H_i represents the radiative heat flux incident on surface zone i, and W_j and $W_{g,j}$ are the radiative fluxes leaving surface zone j and volume zone j, respectively. $E_{g,j}$ $(=\sigma T_g^4)$ denotes the black body emissive power of the volume zone j, and $\omega_o(=\sigma_s/\beta)$ is the scattering albedo of the medium contained in the volume zone j, defined as the ratio of the scattering to total extinction coefficient. Similarly, writing a radiant energy balance on a volume zone i leads to

$$4\beta_i V_i H_{g,i} = \sum_{j=1}^{n}(g_i s_j)W_j + \sum_{j=1}^{m}(g_i g_j)W_{g,j} \qquad (9)$$

where $H_{g,i}$ represents the radiative heat flux incident on a volume zone i. Substituting Equations (7) and (8) for radiosities into radiative energy balances for

volume and surface zones (Equations (6) and (9)), n equations for n surface zones and m equations for m volume zones are obtained.

Simultaneous solution of these n+m equations can be carried out directly for n+m incident fluxes, if the temperatures of each zone are known. Once incident radiative fluxes are available, contributions of surface and volume zones to radiation incident on a surface zone can be calculated by rearranging the first and second summation terms in Equation (6).

$$H_i^S = (1/A_i)\sum_{j=1}^{n}[(s_i s_j)(\varepsilon_j E_j + \rho_j H_j)] \tag{10}$$

$$H_i^G = (1/A_i)\sum_{j=1}^{m}[(s_i g_j)\,((1-\omega_o)E_{g,j} + \omega_o H_{g,j})] \tag{11}$$

where superscripts S and G on H_i denote contributions from surface and volume zones, respectively.

Summation rules for direct exchange areas

Conservation of energy requires that H=W=W_g if all zone temperatures are equal in an enclosure. Thus, Equations (6) and (9) take the following forms

$$A_i = \sum_{j=1}^{n}(s_i s_j) + \sum_{j=1}^{m}(s_i g_j) \tag{12}$$

$$4\beta_i V_i = \sum_{j=1}^{n}(g_i s_j) + \sum_{j=1}^{m}(g_i g_j) \tag{13}$$

These summation rules are useful for checking the calculated direct exchange areas for a given enclosure. If these summation rules are not satisfied then either an error in the calculated energy balance at each zone will arise, or no solution will be found. These rules can also be used in the evaluation of the direct exchange areas. For sufficiently many zones, all exchange areas but one may be calculated by evaluating the integrand between zonal centers, multiplied by the applicable zonal areas and/or volumes. The error made for the closest zones is then offset by applying summation rules for the last one ($g_i g_i$ for volume-volume exchange areas, common-face $g_i s_j$ for volume-surface exchange areas, and common boundary $s_i s_j$ for a corner zone) (Modest, 1993).

Approximation of the Freeboard as a 3-D Rectangular Enclosure

In order to apply the zone method of analysis to the freeboard of the test rig, temperature and radiative properties of the surfaces and the medium must be obtained. The freeboard section of the combustor was treated as a 3-D rectangular enclosure containing gray absorbing, emitting and isotropically scattering medium bounded by diffuse, gray/black walls. The cooler boundary at the top, which consists of gas lanes and cooler tubes, was represented by an equivalent gray surface of effective emissivity and temperature related to area weighted average emissivity and emissive power of the components respectively. The boundary with the bed section at the bottom was represented as a black surface due to the Hohlraum effect (Kozan and Selçuk, 2000). The properties of particle-laden combustion gases were found from Leckner's correlations for participating gases and from the Mie theory for the particle cloud. Details of the approximation of the radiative properties of the participating medium can be found in a recent study by Selçuk et al. (in press).

The radiative properties of the particle-laden combustion gases and the radiative properties and temperatures of the bounding surfaces are given in Table 2. These data, together with polynomials representing medium and side-wall temperature profiles given in Figure 1, provide the input data supplied to the zone method of analysis. The physical system and the treatment of the freeboard is schematically illustrated in Figure 2.

Application of the Zone Method of Analysis

For the application of the zone method to the freeboard of the test rig, the freeboard was subdivided into isothermal volume zones, each of which was assumed to be completely mixed with uniform properties. The surfaces of each volume zone adjacent to the side walls of the freeboard make up a single surface zone with uniform temperature, radiative properties, radiosity, and irradiation. Considering the uniformity of properties throughout the freeboard and absence of steep gradients in temperature and concentration profiles, the freeboard was first subdivided into 10 volume zones, each having dimensions of 0.335 m x 0.45 m x 0.45 m in z, x and y directions, respectively. This subdivision generated 12 surface zones, 10 on the side walls and 2 at

the upper and lower surfaces of the enclosure. The zoning of the freeboard is also illustrated in Figure 2. As a result of this subdivision, 10 radiant energy balances for volume zones and 12 for surface zones have to be solved simultaneously for incident heat fluxes. However, the unknown direct exchange areas present in these balances have to be determined first.

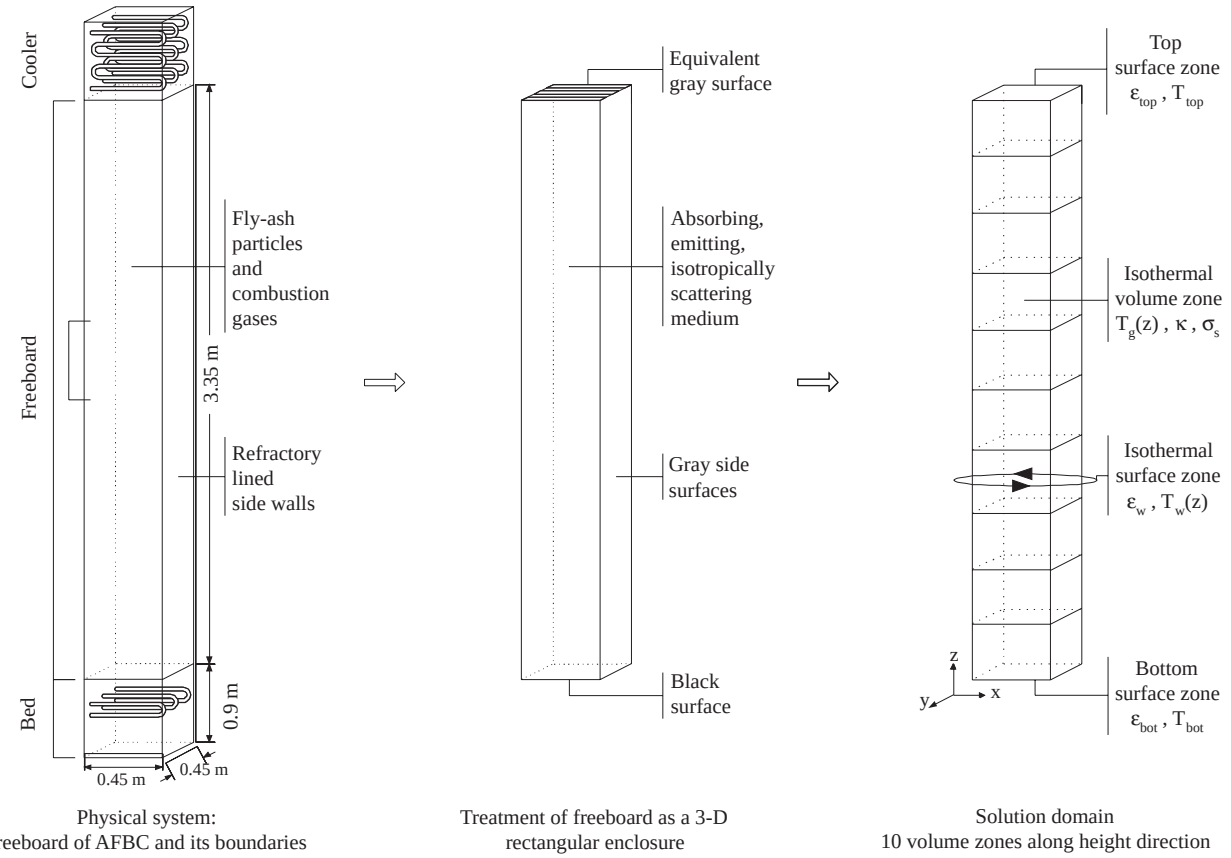

Figure 2. Treatment of the freeboard as a 3-D enclosure and solution domain for the zone method of analysis

Table 2. Radiative Properties of the Medium and the Surfaces

Gas absorption coefficient, κ_g (1/m)	0.43
Absorption coefficient of particle cloud, κ_p (1/m)	0.16
Scattering coefficient of particle cloud, σ_s (1/m)	0.45
Extinction coefficient of the particles, $\beta_p = \kappa_p + \sigma_s$ (1/m)	0.61
Absorption coefficient of the medium, $\kappa = \kappa_p + \kappa_g$ (1/m)	0.59
Extinction coefficient of the medium, $\beta = \kappa + \sigma_s$ (1/m)	1.04
Scattering albedo of the medium, $\omega = \sigma_s \ / \ \beta$	0.43
Emissivity of top surface, ε_{top}	0.87
Emissivity of side surfaces, ε_w	0.33
Emissivity of bottom surface, ε_{bottom}	1.00
Temperature of top surface ($^\circ$ C), T_{top}	549
Temperature of bottom surface ($^\circ$ C), T_{bottom}	873

Direct exchange areas

The determination of direct exchange areas was carried out by direct numerical integration. The accuracy of the integration is a strong function of the size of the differential volume (dV) and/or surface area (dA) appearing in the equations. Hence, finer subdivision of each volume and surface zone into smaller elements is required. Each volume zone, now is subdivided into 10 x 13 x 13 equal-sized smaller volume elements in z, x and y directions, respectively, which leads to 4 x 10 x 13 equal-sized smaller surface elements in each surface zone at the side walls and 13 x 13 elements in the top and bottom surface zones. It must be noted that the number of small elements in all directions was selected in such a way that all the elements are approximately square surface or cubic volume elements. Therefore, the dimensions of the small elements can be represented by the dimension of one side of the surface or volume elements, which is 3.35 cm for the subdivision under consideration. Direct exchange areas between these small volume-volume, volume-surface and surface-surface elements were employed in the determination of direct exchange areas between any zone pairs.

The accuracy of these calculated exchange areas was checked using the summation rules. The absolute percentage error, defined as the ratio of absolute value of the differences between the left-hand sides of Equations (12) and (13) and the right-hand sides to the left-hand sides multiplied by hundred, was found to be a maximum of 5.78. In order to improve the accuracy, direct exchange areas were calculated with a finer subdivision i.e., 20 x 26 x 26 volume and 4 x 20 x 26 surface elements in each volume and side surface zones, respectively. The maximum absolute percentage error was found to be halved in this case. Accuracy was improved further by a subdivision of volume zones to 30 x 40 x 40 smaller elements resulting in a maximum absolute percentage error of 1.91 in the summation rules. Table 3 summarizes the effect of finer subdivision on the errors in the summation rules and CPU times. As can be seen from the table, CPU time increased three orders of magnitude while percentage error decreased but with no change in the order of magnitude as the number of volume elements increases from 10 x 13 x 13 to 30 x 40 x 40. In other words, an improvement in error of only a few percent was achieved at the expense of drastic increase in the CPU time. As the most time consuming step in the prediction of heat fluxes is the calculation of direct exchange areas rather than the solution of radiant energy balances for the zones, CPU time requirement is of utmost importance in setting the number of volume elements in each zone. Considering the accuracy of direct exchange area calculations and computational time required, a 20 x 26 x 26 zone subdivision was found to be optimum for the prediction of heat fluxes at the walls of the freeboard under consideration.

Radiative energy balances

Once the direct exchange areas were available, equations for volume and surface radiant energy balances were solved simultaneously by the Gauss-Jordan elimination method for the unknown incident radiative fluxes. A parametric study on the sensitivity of the predicted incident fluxes to finer subdivision was carried out by running the computer program for 35 volume zones and volume elements of side length 1.367 cm in each volume zone. Average predicted incident radiative heat fluxes for 10 and 35 volume zones was found to differ by 0.7% at the expense of a 33% increase in CPU time. The insensitivity of the predicted heat fluxes to the finer zoning of the enclosure was considered to be due to the absence of steep gradients in temperature profiles and uniform radiative properties within the freeboard.

Table 3. Effects of Finer Subdivision on the Errors in Summation Rules and CPU Time

Number of volume zones	Number of volume elements	Side length of element, (cm)	Max. abs. err. in summation rules, (%)	CPU time ratio*
10	10x13x13	3.350	5.78	0.002
	20x26x26	1.675	2.93	0.086
	30x40x40	1.116	1.91	1.000

* CPU time ratio: CPU time for the case / CPU time for 30 x 40 x 40

* CPU time for 30 x 40 x 40 elements: 107189 seconds on IBM RISC/6000 Model 590

Table 4. Incident Radiative Heat Fluxes on Freeboard Wall

Height (m)	Experimental (kW/m^2)	Predicted (kW/m^2)	Relative Error (%)
1.23	108.9	103.0	5.4
1.83	96.4	102.8	-6.6
2.91	90.2	94.0	-4.2
3.44	71.5	81.8	-14.4
4.19	28.0	51.4	-83.6

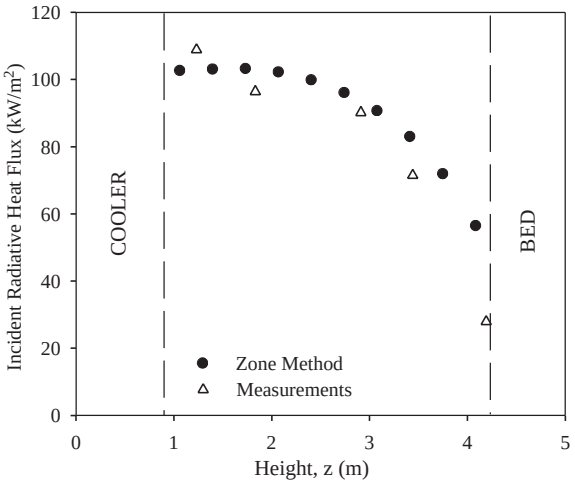

Figure 3. Incident radiative heat fluxes on the freeboard wall

Validation of the model against measurements

In Figure 3 measured and predicted heat fluxes are compared for 10 volume zones with 20 x 20 x 26 volume elements and 12 surface zones. As can be seen from the figure, incident flux decreases from the bed surface toward the cooler and the predictions of model are in good agreement with the measurements.

For comparative testing purposes, point values of the predicted fluxes were compared with the measurements at discrete points. Table 4 shows the relative percentage errors defined as the ratio of predictions subtracted from measurements to measurements multiplied by a hundred. The significant discrepancy between the prediction and the measurement at the uppermost port is considered to be due to the fact that the top surface of the enclosure is approximated by an equivalent gray surface consisting of a cold tube-row/hot gas-lane combination for modeling purposes, whereas the radiometer probe is affected mostly by the cooling tubes as the port for the measurement is located nearly adjacent to a cooler tube.

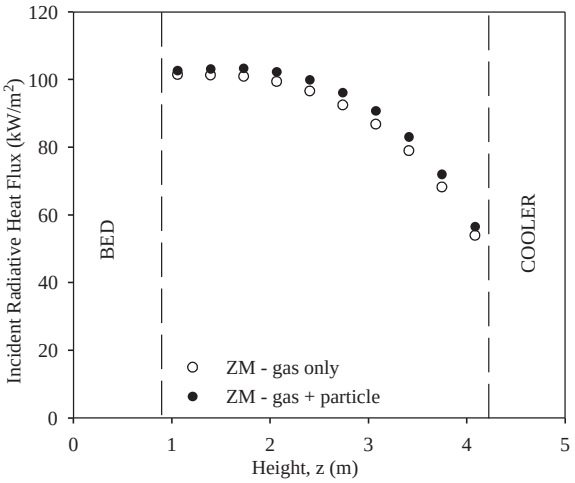

Figure 4. Sensitivity of radiative heat flux to the presence of particles. Gas only: $\beta_p = 0$, gas+particle: $\beta_p = 0.61$

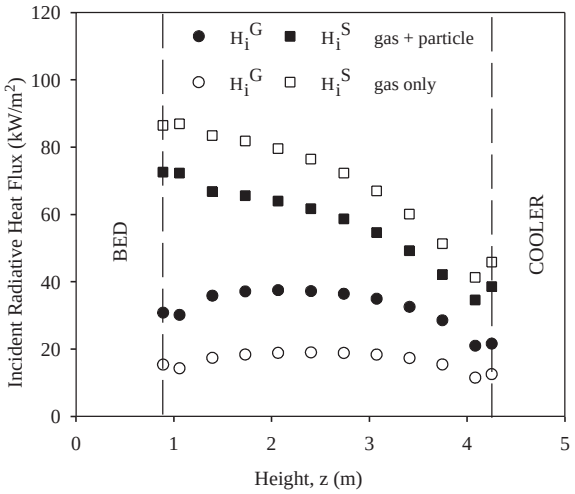

Figure 5. Radiative heat flux incident on a surface zone arriving from volume and surface zones

Sensitivity analysis

The sensitivity of incident heat flux to the presence of particles was analyzed by comparing the predictions of the model with and without particles (Figure 4). As can be seen from the figure, the effect of particles on predicted heat fluxes is negligible. The maximum of the absolute error, defined as

the ratio of difference between predictions with and without particles, to the value with particles which represents the actual physical situation within the freeboard, was found to be 4.6%. This shows that the incident fluxes are relatively insensitive to the presence of particles, which may be considered to be due to low particle loads typically encountered in the freeboards of ABFBCs.

Although the presence of particles does not seem to affect the total radiation arriving at a single surface zone from all other volume and surface zones, the contribution of gas and wall radiation into the fluxes incident on a surface zone is worth illustration. Figure 5 shows the contribution of gas and wall radiation to incident radiation on surface zones along the height of the freeboard in the absence and presence of particles in the combustion gas. As can be seen from the figure, the presence of particles decreases the contribution from surface zones due to the higher extinction caused by the particles whereas it increases the contribution from volume zones due to the absorption of particles in addition to that of gases and hence increase in emissivity of the medium. It is interesting to note that the contribution of radiation from volume zones to total incident fluxes decreased from almost 40% to 20% when the medium was assumed to contain no particles.

Conclusions

Radiative heat fluxes incident on the side walls of the freeboard of an atmospheric bubbling fluidized bed combustor have been predicted by using the zone method of analysis, which is one of the most accurate radiation models available in the literature.

The predictive accuracy of the zone method of analysis was tested by applying it to the prediction of incident radiative fluxes on the walls of the freeboard of an ABFBC and comparing its predictions with measurements. The input data required for the application and validation of the predictions were generated from the METU 0.3 MWt ABFBC test rig operating under steady state conditions. The freeboard containing particle-laden combustion gases was treated as a 3-D rectangular enclosure with gray absorbing, emitting and isotropically scattering medium. The sensitivity of the predicted fluxes to the presence of particles was also analyzed. On the basis of comparisons between predictions and measurements, and the sensitivity analysis, the following conclusions have been reached.

- Incident radiative fluxes at the walls predicted by the zone method reproduce the measured heat fluxes reasonably well.
- The presence of particles in the participating medium does not affect the magnitude of predicted incident fluxes significantly due firstly to the low particle load in the freeboards of bubbling fluidized bed combustors and secondly to the compensation of higher extinction by higher emissivity caused by the particles.

Nomenclature

A	surface area [m^2]
E	blackbody emissive power of a surface [W/m^2]
E_g	blackbody emissive power of a volume [W/m^2]
$g_i g_j$	volume-volume direct exchange area [m^2]
H	radiative heat flux incident on a surface [W/m^2]
H_g	radiative heat flux incident on a volume [W/m^2]
H^G	incident radiative flux on a surface arriving from all volume zones [W/m^2]
H^S	incident radiative flux on a surface arriving from all surface zones [W/m^2]
$s_i g_j$, $g_i s_j$	surface-volume direct exchange area [m^2]
$s_i s_j$	surface-surface direct exchange area [m^2]
T	temperature [K], [$^\circ$ C]
V	volume [m^3]
W	surface radiosity [W/m^2]
W_g	volume radiosity [W/m^2]
ε	surface emissivity [-]
β	extinction coefficient [-]
κ	absorption coefficient [-]
ρ_i	surface reflectivity [-]
σ_s	scattering coefficient [-]
θ	angle of beam between the midpoints of two elements with normal of the elements
ω_o	scattering albedo [-]

Subscripts and superscripts

bottom	bottom surface of the freeboard
f	freeboard
g	gas
p	particle
top	top surface of the freeboard
w	side wall of the freeboard

References

Batu, A., "Modeling of Radiative Heat Tranfer in Freeboard of a 0.3 MW_t AFBC Test Rig Using Zone Method of Analysis", M.S. Thesis, Department of Chemical Engineering, Middle East Technical University, Ankara, Turkey, 2001.

Becker, H.B., "A Mathematical Solution for Gas-to-Surface Radiative Exchange Area for a Rectangular Parallelepiped Enclosure Containing a Grey Medium", J. Heat Transfer, 99, 203-207, 1977.

Filla, M., Scalabrin, A. and Tonfoni, C., "Scattering of Thermal Radiation in the Freeboard of a 1 MW_t Fluidized Bed Combustor with Coal and Limestone Feeding", Twenty-Sixth Symposium (Int.) on Combustion, The Combustion Institute, 3295-3300, Pittsburgh, PA, 1996.

Göğebakan, Y., "Char Attrition in Fluidized Bed Combustors", M.S. Thesis, Department of Chemical Engineering, Middle East Technical University, Ankara, Turkey, 2000.

Hottel, H.C. and Cohen, E.S., "Radiant Heat Exchange in a Gas-Filled Enclosure: Allowance for Nonuniformity of Gas Temperature", AIChE Journal, 4, 3-14, 1958.

Hottel, H.C. and Sarofim, A.F., Radiative Transfer, McGraw-Hill, 1967.

Kozan, M. and Selçuk, N., "Investigation of Radiative Heat Transfer in Freeboard of a 0.3 MW_t AFBC Test Rig", Combustion Science and Technology, 153, 113-126, 2000.

Lindsay, J.J., Morton, W. and Newey, D.C., "Radiative Heat Transfer in the Freeboard Region of a Fluidised Bed", Proceedings of the Fifth Engineering Foundation Conference on Fluidization, Engineering Foundation, New York, NY, 385-392, 1986.

Modest, M.F., Radiative Heat Transfer, McGraw-Hill, New York, NY, 1993.

Noble, J.J., "The Zone Method: Explicit Matrix Relations for Total Exchange Areas", Int. J. Heat Mass Transfer, Vol. 18, 261-269, 1975.

Rhine, J.M. and Tucker, R.J., Modelling of Gas-Fired Furnaces and Boilers, British Gas plc, McGraw-Hill, Great Britain, 1991.

Selçuk, N., Batu, A. and Ayranci, I., "Performance of Method of Lines Solution of Discrete Ordinates Method in Freeboard of a Bubbling Fluidized Bed Combustor", JQSRT (in press).

Smith, T.F., Shen, Z.F. and Alturki, A.M., "Radiative and Convective Transfer in a Cylindrical Enclosure for a Real Gas", J. Heat Transfer, 107, 482-485, 1985.

Truelove, J.S., "Mathematical Modeling of Radiant Heat Transfer in Furnaces", United Kingdom Atomic Energy Authority Report, AERE – R 7817, Chemical Engineering Division, AERE Harwell, Oxfordshire, 1974.

Tucker, R.J., "Direct Exchange Areas for Calculating Radiation Transfer in Rectangular Furnaces", J. Heat Transfer, 108, 707-710, 1986.

Vercammen, H.A.J. and Froment, G.F., "An Improved Zone Method Using Monte Carlo Techniques for the Simulation of Radiation in Industrial Furnaces", Int. J. Heat Mass Transfer, 23, 329-337, 1980.

Viskanta, R. and Mengüç, M.P., "Radiation Heat Transfer in Combustion Systems", Progress in Energy and Combustion Science, 13, 97-160, 1987.